TAKING THE HEAT: IEEE STANDARD 80 AND BIMETALLIC CONDUCTORS

Copyright Material IEEE
Paper No. PCIC-DE-070

Robert D. Southey, P.Eng.
Member, IEEE
SafEngServices & technologies ltd.
3055 Blvd. Des Oiseaux
Laval, Quebec, H7L 6E8
Canada
robert.southey@sestech.com

Jeffrey T. Jordan, P.Eng., MBA
Member, IEEE
Copperweld Bimetallics
5141 Virginia Way
Brentwood, TN 37027
USA
jjordan@copperweld.com

Farid P. Dawalibi, P.Eng., Ph.D.
Senior Member, IEEE
SafEngServices & technologies ltd.
3055 Blvd. Des Oiseaux
Laval, Quebec, H7L 6E8
Canada
farid.dawalibi@sestech.com

Abstract – IEEE Standard 80-2013 provides the substation grounding system designer with simple formulae and tabulated data for the estimation of the maximum fault current that can flow through various types and sizes of conductor, for a given duration, before failure due to fusing occurs. Copper conductors are given exhaustive and reasonably accurate treatment. Other types of conductors, however, are given short thrift. Copper-clad steel (CCS) conductors, whose steel cores provide an effective heat sink, appear not to have been studied at all. As a result, the standard provides only an unrealistic simplified methodology based on fixed physical constants to be used for the calculation of CCS current-carrying limits. Computer modeling and lab testing have demonstrated that the highly non-linear heat absorption characteristics of the CCS core, when properly considered, yield considerably different fault current-carrying capacity than IEEE Standard 80-2013 would lead design engineers to expect. A theoretical framework for the calculation of these values is presented. Computed values are compared with those obtained by an independent accredited high voltage test laboratory.

Index Terms — Copper-clad steel, ampacity, fault current limits, bimetallic conductors, thermal transients

I. INTRODUCTION

Copper-clad steel (CCS) is becoming the material of choice [1-3] for the design of substation grounding systems, due to its much greater current-carrying capacity per unit weight of copper during fault conditions, superior mechanical strength, theft-deterrent properties, and less violent mode of failure, compared with plain copper. Modern CCS conductors can be manufactured to be very finely stranded, resulting in great mechanical flexibility and very effective transfer of I^2R losses from the copper cladding to the steel core, as will be seen. Yet, unlike copper, whose thermal performance when conducting fault current has been extensively studied [4] - [6], with 4 tables of ampacity values dedicated to this material in IEEE Std. 80-2013 [7], steel-cored conductors do not appear to have been given more than fleeting attention. This is possibly because thermal transient calculations involving steel are highly challenging for two reasons: first, steel's thermal characteristics are highly non-linear functions of temperature, with crystalline phase changes occurring below the fusing temperature of copper, as will be seen; second, steel's thermal characteristics vary as a function of carbon content [9] and are not readily available throughout the entire temperature range of interest, i.e., from 20 °C to 1,084.45 °C, the fusing temperature of the copper cladding. Such a material therefore does not lend itself well to simple analytical solutions.

This paper presents the results of laboratory testing of the specific heat of carbon steel samples from one major CCS manufacturer, computer modeling predictions of the current-carrying capacity of CCS based on this and other data available in the published literature, and compares these predictions with high-current laboratory test results of CCS samples subjected to fault current levels near their fusing limits.

II. CALCULATION OF CONDUCTOR AMPACITY

A. Material with Simple Thermal Properties - Copper

IEEE Std. 80 provides a simple formula, Equation 37, to determine the longitudinal rms current, flowing for a given time duration, required to raise the temperature of a cylindrical conductor from ambient temperature to a final, typically fusing, temperature. This equation, derived by Sverak [4], assumes that the conductor's volumetric specific heat remains constant as a function of temperature, that electric resistivity increases linearly with temperature, that heat propagation throughout the cross section of the conductor occurs so quickly that thermal conductivity can be neglected or, equivalently, that current density is uniform throughout the conductor, that no significant heat flows out of the outer conductor surface into the surrounding medium and that skin effect on current distribution can be neglected. These assumptions, while not far off the mark for copper, nevertheless incited Reichman *et al* [5] to develop a more accurate computation method for copper, based on the work of Morgan [6], who assumes that electrical resistivity, conductor density, and specific heat are all second order polynomial functions of temperature, again with skin effect neglected and negligible propagation time of heat through the cross section of the conductor. Reichman *et al* [5] spent considerable effort to carry out extensive high current lab testing of copper samples of various types and sizes and current energizations to validate their computer model, resulting in Tables 3 – 6 in IEEE Std. 80-2013 [7], which yield less conservative predictions than Equations 37 and 47.

B. Material with Complex Thermal Properties - CCS

However, modeling CCS is another matter altogether. Its most notable difference from copper is its steel core, which acts as a

/20/$31.00 © 2022 IEEE

heat sink, thus making it possible to manufacture a high-ampacity conductor with roughly half the amount of increasingly expensive copper. As indicated in Footnote 'd' to Table 1 of IEEE Std. 80-2013, steel "has a highly variable heat capacity from 550 °C to 800 °C… much larger than at lower and higher temperatures...". This can be seen in Fig. 1, which plots the specific heat measured by an independent test lab [10] of three samples of the low-carbon steel core used by one CCS manufacturer, which are compared with the uniform, conservative, specific heat value used in IEEE Std. 80-2013. Clearly, there is some heat absorption that is neglected by the present version of the standard. For comparison, copper has a specific heat of 385 J/kg·°C at room temperature and increases roughly linearly to approximately 530 J/kg·°C at its fusing temperature [6].

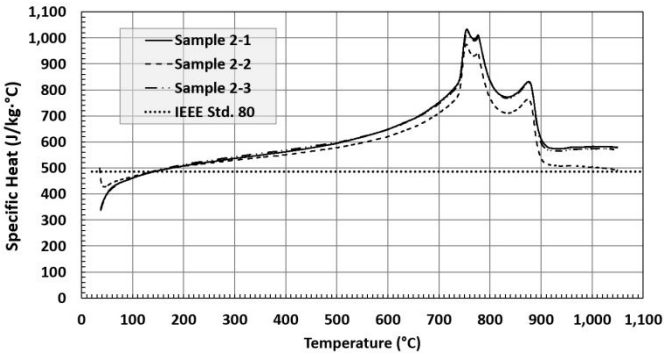

Fig. 1 Measured Steel Specific Heat vs IEEE Std. 80 Value

Steel, of course, is an alloy of iron, carbon, and several other elements. The carbon content alone has a significant impact on the shape of the specific heat curve, as reported by Yafei *et al* [8], which makes it important to test the steel being used for the CCS core. The dual peaks seen in Fig. 1 are due to crystal lattice structure deformations, as discussed in [11] and [12], and these peaks change in width and height with carbon content.

Also dependent on carbon content is steel's thermal conductivity [8], which represents an important CCS cable design consideration. Just as steel has a relatively low electric conductivity, it also has low thermal conductivity of roughly 60 W/m·°C at 0 °C [8] for 0.08% carbon steel, compared with 407 W/m·°C for elemental copper at the same temperature [13]. As a result, as will be seen, there is a non-negligible time delay in the propagation of heat from the copper cladding to the steel core. Thus, the steel, while providing an excellent heat reservoir, is poor at rapidly diffusing heat from its outer surface to its center. This phenomenon is also absent in the treatment of CCS by IEEE Std. 80-2013, which assumes instant propagation of heat throughout the conductor or, equivalently, uniform current distribution throughout the bimetallic conductor. This time-dependent phenomenon also violates one key premise of IEEE Std. 80-2013 Equation 47, namely that $I^2 \cdot t$, the product of time to fusion and the square of the rms current, for a given conductor type and size, is a constant, independent of duration. Another way of putting this claim, in approximate terms, is that the energy required to fuse a CCS conductor is the same, no matter how quickly that energy is delivered to the conductor. This is simply not true, since rapid heating of the copper cladding does not give the steel core time to absorb much heat.

Finally, although the steel core of CCS carries significantly less current than the copper cladding due to its higher electric resistivity, it nevertheless carries a substantial current due to its considerable cross-sectional area. The electric resistivity of steel is decidedly non-linear, as will be seen, making even this aspect of the ampacity calculation defy the implicit assumptions of IEEE Std. 80-2013 Equation 37.

C. New Circuit Method for CCS Temperature Rise Calculation

Despite these challenges, computing the time to fusion of a current-carrying bimetallic conductor such as CCS, with its irregular curves of physical constants versus temperature and two interacting metals, is relatively straightforward with numerical techniques. Indeed, thermal and electrical transient problems satisfy analogous differential equations, lending themselves well to circuit analysis. Cumulative heat, heat flow and temperature are analogous, respectively, to electric charge, electric current and electric potential. Volumetric heat capacity and thermal conductivity are analogous to capacitance and electric conductivity.

Thus, if a cylindrical conductor is subdivided into many thin, concentric, cylindrical shells, as illustrated in Fig. 2, each shell boundary (or the midpoint between a shell's inner and outer boundaries) could represent a circuit node. Heat is generated in each shell by I^2R losses and is also stored in that shell, raising its temperature: the heat generated is modeled as a thermal current injection into that shell, while the heat it stores is thermal charge accumulating on that shell's capacitance with respect to an external reference point.

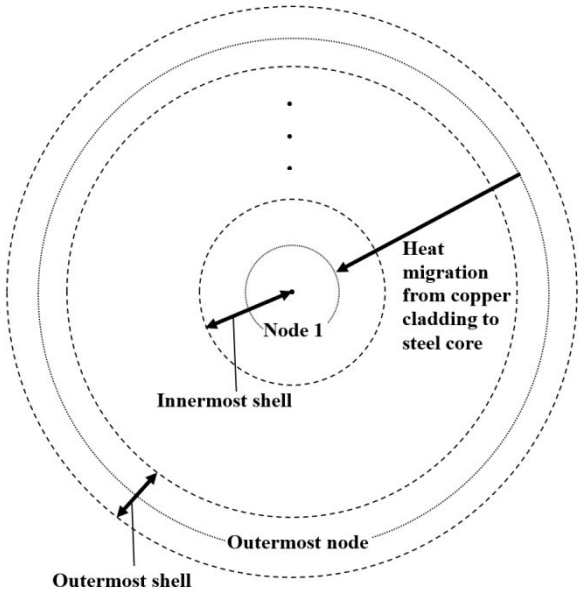

Fig. 2 Concentric Shells and Nodes of Circuit Model

As the charge builds up, the capacitor voltage increases as well. So far, such a model is compatible with the approach used by Reichman *et al* [5], it being understood that the capacitance varies as a function of voltage (i.e., specific heat varies as a function of temperature). However, in CCS, heat flows from the external copper region to the steel core and the propagation time must be considered. Therefore, the new model also considers the flow of heat between concentric cylinders, which is analogous

/20/$31.00 © 2022 IEEE

to the flow of electrical current through a series of resistors, from one shell to the next. Indeed, when one considers the migration of heat from the external surface shell, through the inner shells, to the center of the cable, one can readily imagine a series of thermal resistors, one between each pair of adjacent shells, with a thermal capacitance to ground at each shell or node: i.e., a ladder network. At each node, heat generated by I^2R losses is injected by an ideal current source. The circuit to be solved is illustrated in Fig. 3.

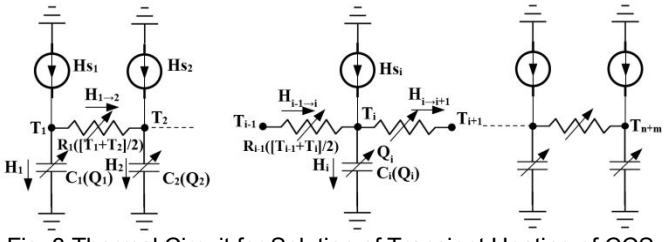

Fig. 3 Thermal Circuit for Solution of Transient Heating of CCS

All physical constants of steel and copper vary with temperature and therefore with time, from one shell to another. As the flow of electric current heats the conductor, therefore, specific heat, density, thermal conductivity, and electric resistivity vary. Each shell is at a different temperature, so all circuit component values change with time and not necessarily at the same rate throughout the CCS conductor. Also, the I^2R losses in each concentric shell vary not only directly with R, but also with the changing distribution of current between shells, as some become hotter and therefore more electrically resistive than others and therefore carry comparatively less current density.

Iterative numerical techniques for the time-domain solution of such transient problems are well known and so will not be discussed in detail here. Suffice it to say that at each point in time, the additional charge on each capacitor is evaluated as a first step, based on the net rate of heat flow into that node computed in the preceding time interval, yielding the new temperature at each node. The resulting thermal voltage or temperature at each node is then used to compute the pertinent thermal circuit model parameters and the electric resistance of each shell, accounting for changes in material density. The total longitudinal current flow in the cable is distributed among the different shells, based on their relative temperature-dependent electric resistances, making it possible to determine the I^2R value to assign to each ideal current source in the thermal circuit model. It then becomes a simple matter to solve the circuit for that time. The time increment used for the present investigation was typically on the order of 0.1 μs and the number of concentric cylinders ranged from 60 to 180, of which 10 to 20 were used for the copper cladding and the remainder for the steel core. In each material, the concentric shells are equally thick.

ASTM B910-07 [14] specifies a nominal value of 9% for the copper cladding thickness as a percentage of the conductor diameter, for 40% conductivity CCS. In practice, however, the thickness of the copper in American-made CCS is closer to 10% or more. The computer simulations described in this paper were therefore carried out with 10% cladding, made of high purity, oxygen-free copper, as required in the manufacturing process to obtain adequate bonding between the copper and the steel.

The physical constants of the copper cladding studied in the present investigation are those of elemental copper, which has a conductivity of 102% IACS at 20 °C. Electric resistivity, specific heat, density and thermal conductivity of copper as a function of temperature were found in Matula [15], Jensen *et al* [16], Jensen *et al* [17], and Hust *et al* [13], respectively. The thermal conductivity data in Hust was limited to temperatures of 300 °K to 1300 °K: these values were linearly extrapolated down to 20 °C and up to 1085 °C and supplemented with an approximate value of 100 W/m·°C for molten copper from Fieldhouse *et al* [18]. The copper was modeled as fusing between 1084.45 °C and 1084.55 °C, to provide a practical means to relate heat absorbed with temperature, with all physical quantities varying linearly between the pre-fusion and post-fusion states.

The physical constants of the 0.06%C carbon steel core of the CCS for which high-current testing was performed were less readily available. The specific heat of three samples was measured by a third-party laboratory [10], using a differential scanning calorimeter, in the temperature range of 35 °C to 1050 °C (see Fig. 1), with temperature increasing at the rate of 20 °C per minute. These values were linearly extrapolated at the high end to 1100 °C; for temperatures below roughly 72 °C, at which spurious noise is clearly seen and was discarded, the average of the three curves was linearly extrapolated down to 20 °C. The curve corresponding to Sample 2-3, which is almost identical to that of Sample 2-1, was retained for the study. Density of SAE 1020 steel, from Clain *et al* [19], was assumed and is believed to be representative of 0.06%C steel. Electric resistivity modeled was for 0.06%C steel in the range of 20 °C to 800 °C, from Yafei *et al* [20], complemented by data in the range of 800 °C to 900 °C for 0.08%C steel, from Colás *et al* [21], and linearly extrapolated to 1,100 °C. Thermal conductivity was obtained from Yafei *et al* [8] for 0.08%C, in the temperature range of 20 °C to 800 °C and linearly extrapolated to 840 °C; for the range of 840 °C to 1100 °C, data for Steel AISI 1020 from Ferreira *et al* [22] was used. While density decreases by only about 4.3% from 20 °C to 1084 °C, the electric resistivity and thermal conductivity vary considerably in this range and in a quite non-linear fashion, as can be seen in Fig. 4.

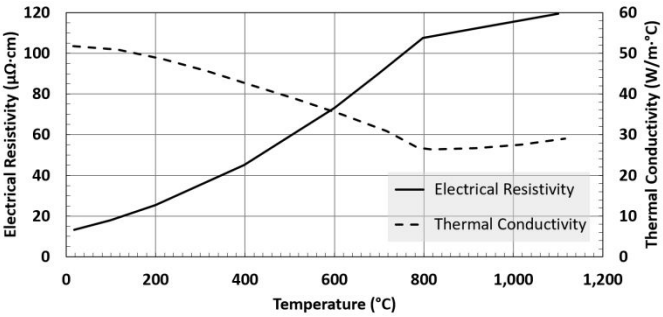

Fig. 4 Electrical Resistivity and Thermal Conductivity of CCS Steel Core Modeled

III. COMPUTER SIMULATION RESULTS

A. Copper Conductors

For validation purposes and to illustrate the difference between the thermal performance of copper and CCS, the new computer model was first applied to 100% IACS copper, using piece-wise linear approximations of the physical characteristics given by the second order polynomials proposed by Morgan [6]. The conductor sizes and symmetrical 60 Hz sinusoidal currents

/20/$31.00 © 2022 IEEE

applied to them were selected from the lab test descriptions given by Reichman *et al* [5].

Three conductor sizes, 1/0, 2/0 and 4/0, were selected, with cross-sectional areas and current magnitudes documented in [5]. The starting ambient temperature was inferred from other tests reported therein. This data is summarized in Table I. Each circuit simulation was run for 0.65 s (past fusion), with 6 500 000 time steps. Each copper strand (19 for the 1/0 and 4/0 conductors, 7 for the 2/0) was subdivided into 60 concentric shells.

TABLE I
COPPER CONDUCTOR SCENARIOS MODELED

Nominal Size	Area (mm²)	Ambient Temp. (°C)	Current (kA)
1/0	54.98	16	22.8
2/0	73.16	16	29.2
4/0	102.16	16	46.9

Table II summarizes the time to reach fusing temperature for each cable size, as estimated by the new circuit model described herein, as computed by Reichman *et al,* and as measured by the latter. As this table shows, the new circuit model prediction is closer to the measured value than that of the Reichman model for the 1/0 conductor, within 0.25% of the Reichman model for the 4/0 conductor and within 2.5% of the Reichman model for the 2/0 conductor, showing good agreement.

TABLE II
COPPER TIME TO FUSING TEMP: COMPUTED VS MEASURED

Nominal Size	Time to Reach Copper Fusing Temperature (s)		
	New Circuit Model	Reichman Model	Reichman Test
1/0	0.5385	0.5310	0.5516
2/0	0.5810	0.5950	0.6076
4/0	0.4390	0.4380	0.4238

Fig. 5 plots the temperature of 7 representative concentric cylindrical shells throughout the 1/0 copper conductor, as a function of time, past fusing, as computed with the circuit model. As can be seen in this graph, the temperature curves are indistinguishable because they all dissipate the same energy per unit cross-sectional area. Note that as the temperature increases, the rate of temperature rise increases also, due to the increasing electric resistivity of the copper.

Let us put the above percent differences between the new circuit model predictions and the Reichman model into perspective, by comparing them with the accuracy of IEEE Std. 80 Equations 37 and 47 in predicting the performance of copper conductors. IEEE Std. 80-2013 Tables 3 – 6 are based on the work of Reichman *et al*, providing ultimate current-carrying capacity for 0.5 s fault durations and 40 °C ambient temperature. Table 6 is applicable to symmetrical sinusoidal waveforms and the other tables to waveforms with a decaying exponential component. The conductor ampacity levels presented in Table 6 are higher than those calculated with Equations 37 and 47 of the standard. For example, for a 4/0 copper conductor (107.2 mm²), Equation 37 yields a fusing current of 42.6 kA and the simplified Equation 47 a fusing current of 42.7 kA, which fall short of the 44 kA value in Table 6 by, respectively, 3.2% and 2.9%. This error is due to the assumption of a heat capacity that does not increase with temperature, mitigated by an underestimate of resistivity at high temperatures due to its assumed linearity. Note furthermore that the error in calculated time to fusion is proportional to the square of the error in ampacity, at least as far as Equations 37 and 47 are concerned, resulting in shortfalls in the fusing time predictions of these two equations of 6.2% and 5.6%, respectively. These values are considerably higher than the 0.25% value cited above for the modeling of 4/0 copper with the new circuit model.

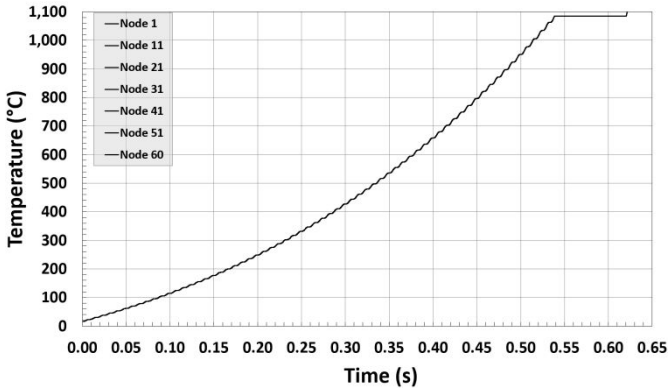

Fig. 5 Temperature Rise of 60 Concentric Copper Shells

B. CCS Conductors

1) *Model Predictions: Thin Strand.* Now consider a 40% conductivity CCS strand, with a diameter of 1.8288 mm (72 mils), with the specific heat given by the Sample 2-3 curve in Fig. 1. A CCS conductor rated for a half-second, 47-48 kA fault current would typically consist of 61 such strands, each of which is assumed to carry an equal share of the total current, i.e., 770-787 A each. When such a strand is modeled in an ambient temperature of 9 °C, energized with 48.1 kA rms, with its steel core subdivided into 50 concentric cylindrical shells and its copper cladding into 10 shells, with a time step size of 0.1 μs, the graph shown in Fig. 6 is obtained. To render the graph legible, only 3 concentric cylinder nodes are shown: Node 1, the center of the steel core, Node 51, the inner surface of the copper cladding, and Node 60, the outer surface of the copper cladding.

As this graph shows, there is no significant temperature difference between the outer and inner surfaces of the cladding, with the steel core lagging, slightly, thanks to the small diameter of each strand, which maximizes the surface-to-volume ratio of the steel core and thus the rate of heat transfer from the copper into the steel. The crystal lattice phase changes in the range of 700 °C to 900 °C can be seen in the unseemly droop in the steel core's temperature curve between these temperatures, where it absorbs more energy per unit temperature rise than elsewhere. Clearly, though, the steel is absorbing heat from the copper, due to the temperature gradient between the two materials. As the graph shows, the copper first reaches its fusing temperature of 1084.45 °C in 480 ms and, based on the linearized assumptions made of the fusing process, takes roughly 32 ms to fuse completely. When the copper cladding thickness is increased to 10.4% of the conductor diameter, which is within manufacturing tolerances, the time to fusing increases to 495 ms. When the copper cladding thickness is maintained at 10%, but the fault current is decreased to 47 kA rms, the time to the start of fusing further increases to 505 ms.

/20/$31.00 © 2022 IEEE

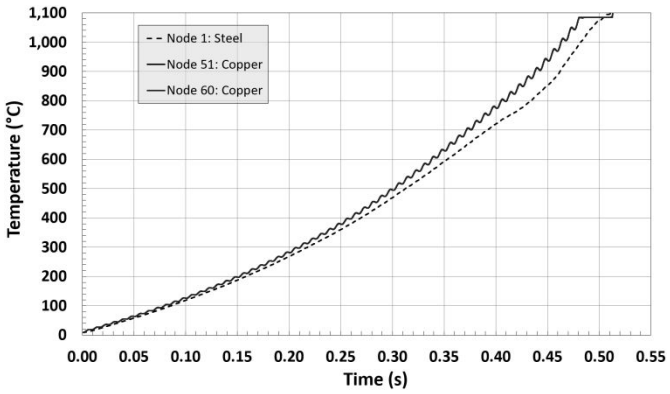

Fig. 6 CCS Temperature Rise: 61 x 1.83 mm Strands, 48.1 kA

2) Lab Testing: Thin Strand. A high current test was carried out at a certified third-party lab [23] on a 1.2 m long sample of such a conductor (40% IACS, 61 x .072" CCS), suspended by oversized lugs 1.2 m above grade, starting at an ambient temperature of 9 °C, and heated with a symmetrical 60 Hz sinusoidal current of 48.1 kA rms, lasting over 500 ms. The start of fusion was detected at 500 ms. This time to fusing is in very good agreement with the new circuit model predictions. Note that the test lab's k=2 expanded uncertainty [24] of the current measuring system was estimated to be 2%, which corresponds to roughly 0.96 kA, showing that the model predictions are well within the accuracy of the laboratory test and manufacturing tolerances.

IEEE Standard 80-2013 Equation 37, when used in conjunction with its associated Table 1, predicts a fusing ampacity value of 44.1 kA, for such a conductor, based on its total cross-sectional area of 160.2 mm^2 (316.2 kcmil), ambient temperature of 9 °C and a duration of 500 ms. This equation underestimates the current-carrying capacity of the CCS conductor by 3 - 4 kA or 6.3% - 8.4%. Unfortunately, there is presently no equivalent to Tables 3-6 for CCS conductors to provide a more accurate rating.

3) *Model Predictions: Large Strand.* Now consider a single CCS strand with the same cross-sectional area as the entire 61-strand conductor described above. The diameter of this strand would be 14.2834 mm (562.3 mils), with an 11.43 mm diameter steel core and a 1.43 mm thick copper cladding, through which a current of 48.1 kA flows, in an ambient temperature of 9 °C. Fig. 7 shows the resulting temperature performance of the cable.

For this larger strand, a larger number of concentric shells were modeled: i.e., 180, with 160 used for the steel core. The results were checked with another model with half as many shells, to ensure that consistent results were obtained. The time step used is still 0.1 μs. As the Fig. 7 shows, although this strand has the same ratio of copper to steel and the same current per unit cross-sectional area as the smaller strand studied, its temperature response is very different, contrary to the IEEE equation predictions, as we shall see.

The most striking difference between Figs. 6 and 7, which would be identical if the assumptions underlying IEEE Std. 80-2013 Equations 37 and 47 were applicable, is the wide spread in temperature between the steel core (Node 1) and the copper cladding (Nodes 161-180), as the cable is heated. Clearly, heat simply cannot flow fast enough from the copper into the bulk of the steel for the entire conductor to have anything resembling a uniform temperature. As a result, the time to the start of fusion of the copper drops from 480 ms, for the thin strand, which can rapidly dissipate heat into its core, to 344 ms, for the large strand, which has nowhere nearly the same steel core surface-to-volume ratio as the thin strand, although both have the same average current density and ratio of copper to steel. On the other hand, IEEE Std. 80-2013 Equation 37 predicts fusing at 420 ms, optimistically overstating the fusing time by 22%.

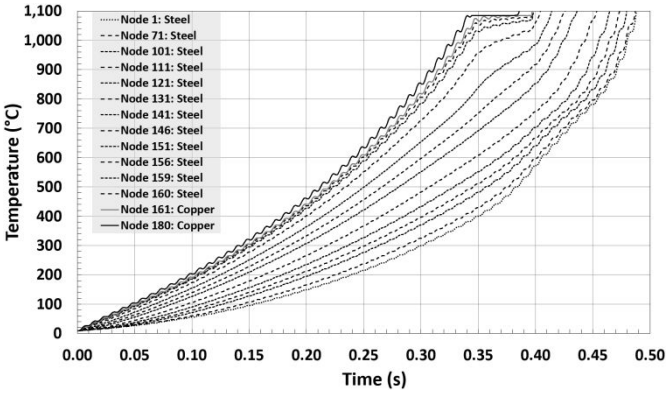

Fig. 7 CCS Temperature Rise: 1 x 14.28 mm Strand, 48.1 kA

Such a large discrepancy is not expected for a material such as copper, in which the current density is much more uniform, resulting in more uniform heating, and whose thermal conductivity is also much greater.

It must be conceded that a single-strand CCS conductor of this size would not normally be encountered, except in the form of a copper-clad steel rod with extra cladding. Nevertheless, similar issues will be encountered with conductors made up of intermediate strand sizes when the ampacity is calculated for shorter fault durations. Consider, for example, the case of a 6 AWG (4.1 mm diameter) 40% CCS single-strand conductor, energized with a symmetrical current of 4.99 kA rms. The computed temperature response is shown in Fig. 8, in which there is a considerable temperature difference between the copper cladding (Nodes 51-60) and the steel core (Nodes 1-50), of which only a representative subset is shown for legibility. The predicted time to start of fusion is 262 ms, according to the new model, with an ambient temperature of 25 °C, as compared with a value of 274 ms, measured by an independent test lab under the same conditions [24]. The predicted time is 4.4% less than the measured time. On the other hand, when the modeled current is decreased to 4.89 kA, which is 2% less, the predicted time to start of fusion increases to 272 ms. Thus, when credit is taken for the 2% uncertainty in the actual test current, the predicted time to fusion is 0.7% from the measured time. IEEE Std. 80 Equation 37 more conservatively predicts an ampacity value of 4.96 kA for a time to fusion of 262 ms. It appears such an optimized combination of large strand size and short clearing time is required for IEEE Std. 80 to yield acceptable results for CCS.

/20/$31.00 © 2022 IEEE

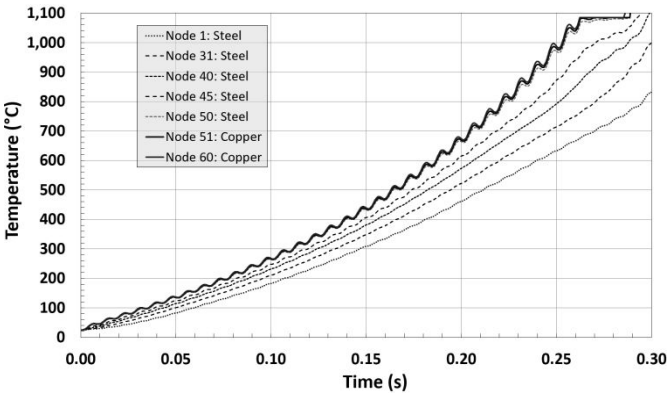

Fig. 8 Single-Strand, 6 AWG 40% CCS, 4.99 kA

IV. APPLICATIONS AND FUTURE WORK

Applying this new circuit method to bimetallic wires will help CCS manufacturers optimize their designs and will provide grounding designers and the IEEE Standard 80 working group a means to compute CCS conductor ampacity more accurately and flexibly. For example, increasing the copper cladding thickness from the 9% nominal value specified in ASTM B910/B910M–07 [14] to 10% of the strand diameter increases the time to start of fusion of a 61 x 1.83 mm CCS wire from 447 to 483 ms, for the same total strand diameter, number of strands, 48.1 kA rms symmetrical current flow and 9 °C ambient temperature.

Calculating time to fusion using a thermal transient circuit model will also be important for grounding system designers in choosing suitable CCS conductors for each application.

Future research work will include tabulating current-carrying limits for CCS for IEEE Std. 80, as a CCS-specific supplement to Tables 3-6.

Future work will also include carrying out further rigorously controlled high-current tests of optimized CCS designs by accredited third-party laboratories, to provide a statistically significant data set for such designs.

V. CONCLUSIONS

This paper presents a new methodology for the prediction of the thermal performance of a complex bimetallic conductor, namely copper-clad steel, accounting for the highly non-linear physical characteristics of steel. This methodology uses a transient time-domain circuit analysis approach, with temperature-dependent circuit components. Thermal properties of low carbon steel are presented, based on a synthesis of data found in the existing literature and new third-party lab testing of the specific heat of representative CCS core samples.

It is shown that the predictions made with this method match those obtained from third-party high-current testing of actual CCS wires, within the accuracy of the lab measurements and manufacturing tolerances of the copper-cladding of the CCS. The new method also successfully predicts the performance of 100% IACS copper conductors. It is further shown that predictions made using the methodology and tables in IEEE Std. 80-2013 for CCS can be highly inaccurate, as they do not realistically represent the specific heat and thermal conductivity of the CCS steel core, underestimating the former and overestimating the latter.

It is shown that the relatively low thermal conductivity of the steel core and its high specific heat mean that the rated fault current of CCS cables is maximized when strand diameter is minimized. On the other hand, large strands experience heat transfer delays to the steel core and therefore reach fusing temperature of the copper cladding more quickly, a phenomenon not predicted by the present IEEE Std. 80-2013 ampacity calculation methodology.

It is hoped that this new knowledge will be put to good use by manufacturers of steel-cored grounding conductors, by grounding designers and by the IEEE Std. 80-2013 working group. This will make it possible to design more robust and theft-resistant grounding systems with considerably less copper, thus potentially reducing costs substantially, while increasing reliability.

VI. ACKNOWLEDGEMENTS

The authors would like to acknowledge contributions to this effort by the following design engineering and test laboratory personnel who helped to develop the data presented in this document: Lora Aboulmouna and Ryan Tosh of Copperweld Bimetallic LLC, Chris Morton, P.Eng., and Qian (Eric) Li, Ph.D., P.Eng., of Powertech Labs Inc., and Dr. Ilir Beta, Ph.D., of ZoCal Thermal Analysis Laboratory.

VII. REFERENCES

[1] Manitoba Hydro, “Sounding Alarm on Copper Heists,” August 2020. Online at https://www.hydro.mb.ca.

[2] J. Chamberlain, “Time To Fight Back: Copper Alternatives Replacing Pure Copper Wire,” Utility Products, Sept 2012. Online at https://www.utilityproducts.com.

[3] P. Tyschenko, R. Riley, and C. Schultz, “Cutting Out Copper Theft,” *T&D World*, Dec. 2010.

[4] J.G. Sverak, “Sizing of Ground Conductors against Fusing,” *IEEE Transactions on Power Apparatus and Systems,* vol. PAS-100, no. 1, pp. 51–59, Jan. 1981.

[5] J. Reichman, M. Vainberg, and J. Kuffel, “Short-Circuit Capacity of Temporary Grounding Cables,” *IEEE Transactions on Power Delivery,* vol. 4, no. 1, pp. 260–271, Jan. 1989.

[6] V.T. Morgan, “Rating of Conductors for Short-Duration Currents,” *Proc. IEE*, Vol. 118, No. 3/4, March/April 1971.

[7] IEEE Std 80-2013, *IEEE Guide for Safety in AC Substation Grounding*, New York, NY: IEEE.

[8] S. Yafei, T. Yongjun, S. Jing and N. Dongjie, "Effect of Temperature and Composition on Thermal Properties of Carbon Steel," *2009 Chinese Control and Decision Conference*, 2009, pp. 3756-3760.

[9] B. R. Teare and J. R. Webb, "Skin Effect in Bimetallic Conductors," in Transactions of the American Institute of Electrical Engineers, vol. 62, no. 6, pp. 297-302, June 1943, doi: 10.1109/T-AIEE.1943.5058713.

[10] I. A. Beta, “Specific Heat Measurement by DSC of Steel Samples,” Report No. 2021-010, ZoCal Thermal Analysis Laboratory, Fayetteville, TN, December 13, 2021.

[11] J. H. Awbery and E. Griffiths, “The Thermal Capacity of Pure Iron,” *Proc. R. Soc. Lond.*, vol. 174 A, pp 1-15, Jan. 1940.

/20/$31.00 © 2022 IEEE

[12] J. L. Dossett and H. E. Boyer, *Practical Heat Treating*, ASM International, 2nd Ed., Chapter 2, 2006.
[13] J. G. Hust and A. B. Lankford, *Thermal Conductivity of Aluminum, Copper, Iron, and Tungsten for Temperatures from 1 K to the Melting Point,* U.S. Dept. of Commerce, National Bureau of Standards, June 1984.
[14] ASTM B910/B910M–07, *Standard Specification for Annealed Copper-Clad Steel Wire*, ASTM International, West Conshohocken, PA, Reapproved 2013.
[15] R. A. Matula, "Electrical Resistivity of Copper, Gold, Palladium, and Silver", *Journal of Physical and Chemical Reference Data 8*, pp 1147-1298 (1979).
[16] J. E. Jensen, W. A. Tuttle, R. B. Stewart, H. Brchna, and A. G. Prodell, *Brookhaven National Laboratory Selected Cryogenic Data Notebook, Volume I, Section 8*, revised August 1980.
[17] J. E. Jensen, W. A. Tuttle, R. B. Stewart, H. Brchna, and A. G. Prodell, *Brookhaven National Laboratory Selected Cryogenic Data Notebook, Volume I, Section 14*, revised August 1980.
[18] I. B. Fieldhouse, J. C. Hedge, J. I. Lang JI, and T. E. Waterman, *WADC Technical Report 55–495, Part II. AD.* 1956; 110510:1–18.
[19] F. Clain, P. Teixeira, and D. Araújo, "A Heat Source Model to Simulate Welding Processes with Magnetic Deflection," ENCIT 2016 – 16th Brazilian Congress of Thermal Sciences and Engineering.
[20] S. Yafei, N. Dongjie and S. Jing, "Temperature and Carbon Content Dependence of Electrical Resistivity of Carbon Steel," *2009 4th IEEE Conference on Industrial Electronics and Applications*, 2009, pp 368-372.
[21] R. Colás and G. E. Totten (Ed.), *Encyclopedia of Iron, Steel, and Their Alloys*, CRC Press, 2016, p 1837.
[22] D. M. Ferreira, A. Silva Alves, R. Cruz Neto, T. Ferreira Martins, and S. D. Brandi, "A New Approach to Simulate HSLA Steel Multipass Welding through Distributed Point Heat Sources Model," *Metals - Open Access Metallurgy Journal*, 2018.
[23] C. Morton, Q. Li, "Copper and CCS Withstand Current and Fusing Current Tests," *Powertech Labs Inc. Report ID PL-03027 REP1*, April 2020.
[24] National Institute of Standards and Technology, "Uncertainty of Measurement Results," last update December 2017. Online at https://physics.nist.gov/cuu/Uncertainty/coverage.html.
[25] C. Morton, Q. Li, "6 AWG Wire Fusing Current Test," *Powertech Labs Inc. Report ID PL-02227 REP1*, October 2018.

VIII. VITAE

Robert D. Southey, P.Eng., graduated from McGill University in 1986, with a B. Eng. degree (honors – electrical). He has worked for SES ltd. ever since, as a researcher, engineer, project manager, and applied R&D department director, specializing in grounding-related measurement techniques, electrical safety studies, power system grounding, AC interference analysis and mitigation, and transient analysis. Mr. Southey has written over 250 technical reports and over 50 technical papers and articles, references to which are made in IEEE Standards 80 and 81. Mr. Southey has also participated in the task groups responsible for developing NACE International SP0177 and SP21424. He is a registered professional engineer in the Provinces of Quebec, Manitoba, Alberta, and Ontario, Canada.

Jeffrey T. Jordan, P.Eng., M.B.A, graduated from the University of Michigan with a Bachelor of Science-Engineering degree in 1995 and Vanderbilt University with a Master of Business Administration in 2014. He has led ship design activities for the U.S. Navy and the National Science Foundation. He has also led research and development activities for Square D and Schneider Electric, supervising over 5,000 hours of high-power laboratory test activities. He is currently the Power Grid Product Manager for Copperweld Bimetallic LLC, the leading manufacturer of engineered bimetallic wire and cable solutions, living and working in the greater Nashville TN area.

Farid P. Dawalibi, P. Eng., graduated from Ecole Polytechnique de Montréal, Montreal, QC, Canada with M.Sc. (1973) and Ph.D. (1978) degrees in electrical engineering. From 1971 to 1976, he was a Consulting Engineer with Shawinigan Engineering Company, Montreal, QC, Canada, where he worked on numerous projects involving power system analysis and design, railway electrification studies, and specialized computer software code development. In 1976, he joined Montel-Sprecher&Schuh, Montreal, QC, Canada, a manufacturer of high-voltage equipment, as Manager of Technical Services and was involved in power system design, equipment selection, and testing for systems ranging from a few to several hundred kilovolts. In 1978, he founded Safe Engineering Services & technologies ltd., Laval, QC, Canada, a company that specializes in soil effects on power networks. Since then, he has been responsible for the engineering and software development activities of the company. He has authored more than 300 papers on power system grounding, lightning, inductive interference, and electromagnetic field analysis. He has also written several research reports for the Canadian Electricity Association and the Electric Power Research Institute. He is a registered professional engineer in the Provinces of Quebec and Manitoba, Canada.

/20/$31.00 © 2022 IEEE